

# A new tunneling path for reactions such as $\text{H} + \text{H}_2 \rightarrow \text{H}_2 + \text{H}^{\text{a}}$

R. A. Marcus and Michael E. Coltrin

Department of Chemistry, University of Illinois, Urbana, Illinois 61801  
(Received 20 May 1977)

The standard tunneling path in transition state theory for reactions such as  $\text{H} + \text{H}_2 \rightarrow \text{H}_2 + \text{H}$  has been the so-called reaction path, namely the path of steepest ascent to the saddle point. This path is now known to give numerical results for the reaction probability which are in disagreement with the exact quantum mechanical ones by an order of magnitude at low tunneling energies. A new tunneling path corresponding to a line of vibrational endpoints is proposed. It is much shorter and is shown to give results in agreement with the quantum ones to within about a factor of two. A semiclassical basis for choosing this new path is given.

## I. INTRODUCTION

Recent comparisons of quantum mechanical and transition state theory calculations for the colinear and three-dimensional reaction rates of  $\text{H} + \text{H}_2 \rightarrow \text{H}_2 + \text{H}$  have revealed significant discrepancies between the two methods.<sup>1</sup> These discrepancies occur particularly at low energies, where tunneling is very important. The quantum mechanical rate is frequently of the order of ten to a hundred times larger than the rate predicted by transition state theory. Various numerical complex-valued classical trajectory studies have been made in this tunneling region, and used in semiclassical calculations<sup>2,3</sup> and more recently in a periodic-trajectory-transition-state (PTTS) formalism.<sup>4</sup> The results obtained using the PTTS show markedly improved agreement with the quantum mechanical results.<sup>4</sup> (The semiclassical ones did also, but they are not of the transition state theory type.)

The question arises whether there is some simple physically intuitive modification of the usual tunneling calculation in transition state theory which yields good agreement, without requiring the computation of actual classical trajectories. Such a method is described in the present paper. It involves a new tunneling path for this  $\text{H} + \text{H}_2 \rightarrow \text{H}_2 + \text{H}$  reaction, a path corresponding to the vibrational limit during the motion. A semiclassical basis for the method is given.

## II. TUNNELING PATH AND RESULTS

In transition state theory<sup>5</sup> it is customary to calculate the "reaction path," the curve of steepest descent passing through the saddle-point, and employ it as the tunneling path. We let the coordinates along that path be denoted by  $s$ , and the potential energy along this "s-curve" by  $V_1(s)$ . For a colinear reaction in the tunneling region the vibrational energy of the lowest vibrational state in the transition state at  $s = s^\ddagger$  is the zero-point energy,  $E_0(s^\ddagger)$ . The translational energy available for tunneling at any  $s$  is then often chosen to be the total energy  $E$  minus  $V_1(s) + E_0(s^\ddagger)$ . Actually, the effective potential energy barrier is  $V_1(s) + E_0(s)$ , where  $E_0(s)$  is the system's local zero-point energy at a given  $s$ , and this barrier is now frequently used instead of  $V_1(s) + E_0(s^\ddagger)$ . Classical-

ly, the system will stop its motion in the  $s$ -direction at the  $s = s^*$  for which the energy barrier equals the total energy, i. e., for which

$$V_1(s^*) + E_0(s^*) = E, \quad (2.1)$$

for a system in its lowest vibrational state.

The coordinate perpendicular to the  $s$ -curve, a vibrational coordinate, is denoted by  $\rho$ , with  $\rho$  positive when this coordinate is stretched, and negative when compressed.  $\rho$  equals a (signed) measure of the distance perpendicular to a tangent to the  $s$ -curve. The potential energy associated with  $\rho$ -motion at any  $s$  is designated  $V_2(\rho, s)$ , where  $V_2(0, s) = 0$  on the  $s$ -curve. The maximum vibrational amplitude at a given  $s$  is the  $\rho = \rho_{\text{max}}$  which satisfies

$$E_0(s) = V_2(\rho_{\text{max}}, s). \quad (2.2)$$

The family of points  $[\rho_{\text{max}}(s), s]$  satisfying (2.2) and for which  $\rho$  is positive describes a curve, which we shall call the  $t$ -curve.

The contour lines of a typical potential energy surface for the  $\text{H} + \text{H}_2$  reaction are depicted using the usual skewed axes<sup>5</sup> in Fig. 1. The reaction path (the  $s$ -curve) is shown as a solid line, and the  $t$ -curve as the dotted line. The central idea of the present paper is that a preferred way of tunneling is not along the reaction path, the  $s$ -curve, but rather along a shorter path, the  $t$ -curve described above. The tunneling along the  $t$ -curve starts from a point  $P$  for which  $s = s^*$  and  $\rho = \rho_{\text{max}}$  and continues along the  $t$ -curve to a corresponding point  $P'$  in the exit channel, i. e., the point for which (2.1) and (2.2) are again satisfied but in the exit channel in Fig. 1. The starting and end points on the  $t$ -curve,  $P$  and  $P'$ , depend on the energy  $E$ , as in (2.1), and are given in Fig. 1 for a particular  $E$ . If  $V$  denotes the potential energy along the  $t$ -curve then

$$V = V_1(s) + E_0(s) \quad (\text{on } t\text{-curve}), \quad (2.3)$$

as compared with  $V_1(s)$  on the  $s$ -curve.

If  $dq$  denotes an element of length along the tunneling path, then the imaginary part of the complex-valued phase integral which appears in a tunneling calculation is  $J(E)$ ,

$$J(E) = \text{Im} \int_P^{P'} p dq / \hbar \quad (2.4)$$

<sup>a</sup>Supported by a grant from the National Science Foundation.

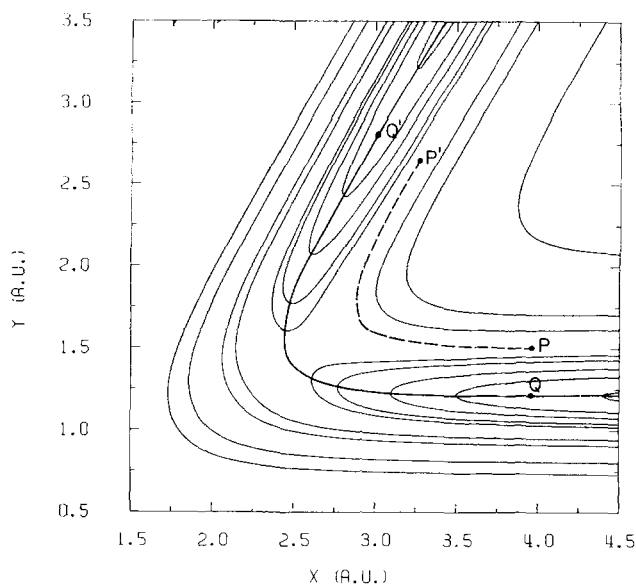


FIG. 1. Plot of potential energy contours for the  $\text{H} + \text{H}_2 \rightarrow \text{H}_2 + \text{H}$  reaction using the Porter-Karplus surface. Solid line is line of steepest ascent (reaction path). Dotted line is the  $t$ -curve (limit of vibrational amplitudes in the given vibrational state, here the zero-point state). The points  $P$  and  $P'$  denote the initial and final tunneling points on the  $t$ -curve for a particular total energy. The corresponding tunneling points if tunneling occurred along the reaction path are  $Q$  and  $Q'$ .

where  $\text{Im}$  denotes "imaginary part of";  $p$  is the component of the momentum along the path, e. g., on the  $t$ -curve it is

$$p = [2\mu(E - V)]^{1/2}, \quad (2.5)$$

where  $V$  is given by (2.3).  $\mu$  is a reduced mass whose value depends on the distance scaling factors used in

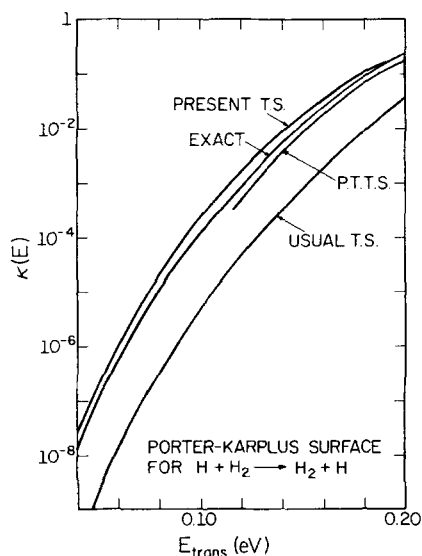


FIG. 2. Plot of reaction probability vs initial translational energy in the center of mass system for the  $\text{H} + \text{H}_2 \rightarrow \text{H}_2 + \text{H}$  reaction, for the Porter-Karplus potential energy surface. Curves are given for the exact quantum mechanical result (Ref. 9), the usual transition state theory result, the present transition state theory result and a result (PTTS) which introduces numerically computed periodic trajectories into a transition state theory [curve from Fig. 6 of Ref. 4(b)].

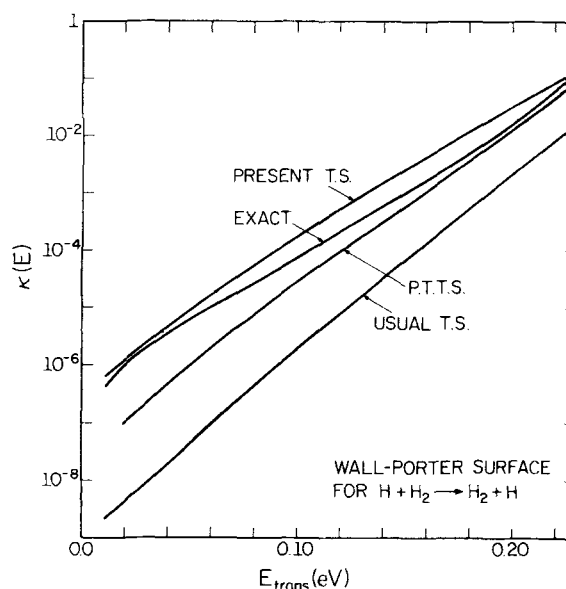


FIG. 3. Same legend as Fig. 2, but for an SSMK Wall-Porter potential energy surface. Exact results are from Ref. 10(b) and the PTTS curve is obtained from Fig. 5 of Ref. 4(b).

Fig. 1. The  $\mu$  and scaling factors used in the present paper are the standard ones.<sup>5,6</sup>

The semiclassical transmission coefficient (ratio of outgoing flux of products to incident flux of reactants) is  $\kappa(E)$ . Using the results obtained by mapping the effective potential onto one of parabolic form,  $\kappa(E)$  is given by<sup>7</sup>

$$\kappa(E) = \exp(-2J) / [1 + \exp(-2J)]. \quad (2.6)$$

The initial translational energy is  $E - E_0(-\infty)$ , where  $E_0(-\infty)$  is the initial zero point energy. A plot of  $\kappa(E)$  versus this translational energy, for the Porter-Karplus surface<sup>8</sup> and for the new tunneling path, is shown in Fig. 2, together with the quantum mechanical<sup>9</sup> and conventional transition state results. The results are seen to agree quite well with the quantum ones,<sup>9</sup> and show considerable improvement over the use of the conventional path. In Fig. 3 the corresponding results for the SSMK Wall-Porter surface<sup>10,11</sup> are shown. The results agree with the quantum results<sup>10(b)</sup> to about the same accuracy as before. An interesting approach to transition state theory, given by Miller<sup>4</sup> *et al.*, utilizes numerically computed classical trajectories (periodic-trajectory-transition-state method, PTTS). The results are given in Figs. 2 and 3.

In the  $\text{H} + \text{H}_2 \rightarrow \text{H}_2 + \text{H}$  reaction at the total energies given in Figs. 2 and 3 no excited vibrational states of  $\text{H}_2$  can exist. In other systems for which excited vibrational states can exist in this tunneling region, one can compute a transmission coefficient  $\kappa_n(E)$  for the  $n$ th vibrational state at the given total energy, using (2.6) with  $E_0(s)$  in (2.1)–(2.3) replaced by  $E_n(s)$ . The sum of the transmission coefficients at the total energy  $E$  is then the sum  $\sum_n \kappa_n(E)$  over all energetically accessible initial states  $n$  in a microcanonical ensemble of initial states. Microcanonical transition state theory, and the manner in which each  $\kappa_n$  contributes to the reactive flux is de-

scribed, in both the adiabatic and general forms of microcanonical transition state theory in Ref. 12.

A theoretical basis for the present choice for the tunneling path is obtained from the semiclassical arguments given in the next section.

### III. SEMICLASSICAL ARGUMENTS

In semiclassical theory the action variables are the classical analog of the quantum numbers.<sup>13(a)-13(f)</sup> One can obtain a wavefunction<sup>13(c),13(d)</sup> for a collision system beginning in a given specified initial quantum state  $n$ , by using a set of classical trajectories having the desired initial action variables but uniformly distributed in initial phase  $\bar{w}_0$ . When this wavefunction is introduced into a well-known quantum mechanical expression for the  $S$ -matrix elements  $S_{mn}$  one obtains an integral expression for these elements.<sup>13(d),13(e)</sup> The reaction probability (transmission coefficient) of a system in state  $n$  is

$$\kappa_n = \sum_m |S_{mn}|^2, \quad (3.1)$$

where the sum is over all final states  $m$  of products. The  $S$ -matrix element can be written as (3.2) for a two coordinate system (the  $\bar{d}\bar{w}^0$  becoming  $\bar{d}\bar{w}_1^0 \bar{d}\bar{w}_2^0 \dots$ , and the preexponential factor becoming a determinant, for a higher dimensional system):<sup>13(d)</sup>

$$S_{mn} = \sum_{\text{paths}} \int_{\bar{w}^0=0}^1 |\partial \bar{w} / \partial \bar{w}^0|^{1/2} \exp \left[ -i \int_{p^i}^{p^f} q dp \right. \\ \left. + 2\pi i (\bar{n} - m) \bar{w} - N\pi i \right] \bar{d}\bar{w}^0, \quad (3.2)$$

where  $\bar{w}$  is a final angle variable (a final phase), a constant for any trajectory,  $\int q dp$  denotes a path integral with  $q$  being a distance along the path if the coordinates are Cartesian, and  $p$  being the local Cartesian momentum component along the path. (If other coordinates are used  $q dp$  denotes a sum  $\sum_k q_k dp_k$  over all coordinates  $k$ .) The integration limits are from the value ( $p^i$ ) of the momentum  $p$  at a vibrational endpoint at some large initial separation distance  $R^i$  to that ( $p^f$ ) at a vibrational endpoint at some final separation  $R^f$ . The integration path is chosen to consist of three parts: first at a fixed  $R (= R^i)$  from the vibrational end-point to some desired initial vibrational phase  $\bar{w}^0$ , then along an actual classical trajectory to the final specified separation distance  $R^f$  (in the present case in the products' channel) and final phase  $\bar{w}$ , and then at fixed  $R^f$  to a vibrational endpoint at the  $R^f$ . The first and third legs of the integration are performed in regions where the internal motion is separable from the translational motion, and so an integration path at fixed  $R$  can be chosen in those regions.  $N$  is related to the number of times the trajectory touches one of the vibrational caustics (the one not joining the initial and final vibrational endpoints).<sup>12(d)</sup> The classical mechanical analog of the final quantum number of the trajectory in the products' channel is  $\bar{n}$ , and the transition of interest for  $S_{mn}$  is for  $n \rightarrow m$ .

The principal approximation which will be introduced into (3.2) is one of vibrational adiabaticity, namely the assumption that the quantum number  $n$  remains constant

during the trajectory.<sup>14</sup> The assumption presumes a high enough vibrational frequency of the motion transverse to the reaction path. With the assumption of vibrational adiabaticity, the value of the classically attainable  $s$  becomes independent of the initial vibrational phase  $\bar{w}^0$ . This  $s^*$  is then given by Eq. (2.1) in the case that the vibrational state is the lowest one (and by the same equation with  $E_0(s^*)$  replaced by  $E_n(s^*)$ , when the vibrational state is any given state  $n$ ). These trajectories thereby each reach the same vibrational turning point  $P$  at  $s^*$ , and then tunnel from there since it is the closest point to the classically allowed region of the products' channel. Thereby, for each  $\bar{w}^0$  one has the same value of the complex-valued quantity  $\int p dq$  in (3.2) from point  $P$  to point  $P'$  for each member of this family of trajectories, a family whose members differ only in  $\bar{w}^0$ .

In Eq. (3.2) one can now set  $\bar{n} = n$ , since in the vibrationally-adiabatic approximation all trajectories will have the same value of  $\bar{n}$ , namely the initial value  $n$ . (When the coordinates  $\bar{d}\bar{w}^0$  denotes  $\bar{d}\bar{w}_1^0, \bar{d}\bar{w}_2^0, \dots, \bar{n}$  and  $n$  denote  $\bar{n}_1, \bar{n}_2, \dots$  and  $n_1, n_2, \dots$ ). The integral over  $p$  can be integrated by parts, yielding  $\int p dq - p_R^f R^f + p_R^i R^i$ ,  $p_R$  being the translational momentum, since the vibrational momentum vanishes at the end points of the above integration path.  $p_R^f$  and  $p_R^i$  are the final and initial translational momenta. The trajectories beginning with different  $\bar{w}^0$  will all have the same value for this integral because of the absence of a relative distortion of the trajectories in a vibrationally-adiabatic approximation. It can then be placed outside the integral over  $\bar{w}^0$ . Because of this lack of distortion the  $\partial \bar{w} / \partial \bar{w}^0$  in (3.2) can be set equal to unity. If the imaginary part of  $\int p dq / \hbar$ , namely the value along the path between  $P$  and  $P'$ , is denoted by  $J(E)$ , Eq. (3.2) gives (3.3) for  $|S_{mn}|^2$ , after integration over  $\bar{w}^0$ ,

$$|S_{mn}|^2 = \exp(-2J). \quad (3.3)$$

Equation (3.3) presumes only a single traverse between points  $P$  and  $P'$ , whereas one should really sum in the right hand side of (3.2) over all traverses, as indicated by  $\sum_{\text{paths}}$  (suitably renormalized to conserve flux, when there is a branching of the paths). For example, the system may go from  $P$  to  $P'$ , and return to the reactants' channel, or go from  $P$  to  $P'$ , return to  $P$ , return to  $P'$ , and then go into the products channel, and so on. There are an infinite number of such paths. In effect, a sum over all these paths is obtained by mapping the tunneling problem between  $P$  and  $P'$  onto the parabolic barrier problem, and solving that problem, with the result that the tunneling factor is given<sup>7</sup> by (3.4) instead of (3.3).

$$|S_{mn}|^2 = \exp(-2J) / [1 + \exp(-2J)] \quad (3.4)$$

Eq. (3.4) reduces to (3.3) when  $J$  is large, that is when all paths but the single traverse path become unimportant.

To summarize, we have introduced into (3.2) the approximations of vibrational adiabaticity and a semiclassical tunneling expression (3.4), with the implication of tunneling along the shortest path, namely between  $P$  and  $P'$ . The tunneling approximation (3.4) should introduce very little error, since it has been numerically

tested. The third and final approximation which remains to be introduced is the choice of the optimum tunneling path between  $P$  and  $P'$  for calculating  $J$ . The "best" path is a dynamical one, namely the one which, by Hamilton's principle of least action, has the least value of  $\int p dq$  between the two points.<sup>15(b)</sup> We have selected the  $t$ -curve, the  $t$ -curve being one which involves tunneling in the  $s$ -direction and not in the  $\rho$ -direction. We have indeed examined a number of other paths and found the  $\text{Im} \int p dq$  for those paths for the present reaction either to have nearly the same or a larger value. Examples are given in Appendix A.

A principal assumption, as already noted, is the vibrational adiabatic one. Actually, any reaction, even  $\text{H} + \text{H}_2 \rightarrow \text{H}_2 + \text{H}$ , is at least somewhat vibrationally-nonadiabatic.<sup>14</sup> For example, classical trajectories for this reaction reveal that  $s^*$  depends somewhat on  $\bar{w}^0$ .<sup>16</sup> Thus, as a result of passing through the pretransition state region there has been some change in the vibrational action variable of the  $\rho$ -motion before reaching  $s^*$ , whereas that action variable would be constant in a vibrational-adiabatic approximation. Thereby, for some  $\bar{w}^0$ 's the  $s^*$  is larger and for others smaller than that determined by Eq. (2.1). We have termed this vibrational nonadiabaticity elsewhere the "nonadiabatic tail,"<sup>17</sup> because some systems will pass over the barrier at energies where in the vibrationally-adiabatic approximation they could not. The agreement in Figs. 2 and 3 is nevertheless seen to be quite reasonable.

#### IV. DISCUSSION

The new tunneling path is a simple path which provides a considerably improved agreement with the quantum results, as compared with the standard tunneling path. We have neglected vibrational-nonadiabaticity in the pretransition state region, as indeed do all quantum transition state theories. Vibrational nonadiabaticity allows some systems to pass  $s^\ddagger$  with a vibrational energy less than  $E_0(s^\ddagger)$ , and causes any transition state theory results at energies near  $E$  equal to  $V(s^\ddagger) + E_0(s^\ddagger)$  to be too low. The error is not more than a factor of about two, judging from the results in that region (largely not given in Figs. 2-3, but calculated).<sup>18</sup>

We have considered above a class of reactions involving three centers of comparable (in the present case equal) masses. One system of particular interest is the transfer of a light particle between two heavy ones. Here, the acute angle in Fig. 1 is so much smaller that the exit and entrance channels are almost parallel. Dynamically this system is quite different, and it is planned to discuss tunneling for such a system elsewhere.

Finally, we should note that tunneling along a path other than the standard reaction path was first employed by Johnston and Rapp,<sup>19</sup> who considered straight line paths.

#### ACKNOWLEDGMENT

We are pleased to acknowledge the support of this research by the National Science Foundation. One of us

(M. E. C.) was the recipient of a University of Illinois Fellowship.

#### APPENDIX A. ACTION CALCULATED ALONG ALTERNATIVE TUNNELING PATHS

We consider the phase integral  $\int_P^{P'} p dq$  along several paths to compare with the value along the  $t$ -curve. The principle of stationary action for fixed  $P$ ,  $P'$ , and  $E$  is

$$\delta \int_P^{P'} p dq = 0, \quad (\text{A1})$$

which implies that the variations (from the value along the best dynamical path) of its real part and of its imaginary part are zero. The latter part determines the tunneling probability [cf. Eq. (3.3)], and we focus attention on it. Strictly speaking, the  $p$  in (A1) should be directed along that path. We first consider some paths for which this is not the case but which satisfy vibrational adiabaticity.

One family of curves is the following: (1) a path at constant  $s^*$  from  $\rho = \rho_{\text{max}}$  to  $\rho = k\rho_{\text{max}}$  where  $k$  is a constant less than unity, (2) a path with  $\rho(s) = k\rho_{\text{max}}(s)$  from that  $s^*$  to the  $s^*$  in the exit channel, and (3) a path at that  $s^*$  from  $\rho = k\rho_{\text{max}}$  to  $P'$ . Only step (2) contributes to  $\text{Im} \int p dq$ , when  $\rho$  lies between its minimum and maximum classically allowed values. At any point in step (2) the relevant value of  $p$ ,  $p_s$ , in the integrand (the component along the path) is  $\{2\mu[E - E_0(s) - V_1(s)]\}^{1/2}$ , since

$$(p_s^2/2\mu) + E_0(s) + V_1(s) = E. \quad (\text{A2})$$

Thus, at any  $s$  in step (2) the  $p$  in the integrand, namely  $p_s$ , is the same as the  $p$  on the  $t$ -curve, given by Eqs. (2.3) and (2.5). However, the path along step (2) is longer than that along the  $t$ -curve, and thus the value of  $\text{Im} \int p dq$  is greater than that along the  $t$ -curve. For example, for the SSMK Wall-Porter surface at  $E = 0.3985$  eV,  $J(E)$  along the  $s$ -curve is 5.81, whereas that along the  $t$ -curve is only 3.65. ( $J$  is  $\text{Im} \int p dq/\hbar$ .)

Another set of paths is that for which  $\rho(s) \geq \rho_{\text{max}}(s)$ . Once again we first choose a three-step path: (1) a path at the initial  $s^*$  from  $\rho = \rho_{\text{max}}$  to  $\rho = k\rho_{\text{max}}$ , where  $k$  is a constant greater than unity, (2) a path with  $\rho(s) = k\rho_{\text{max}}(s)$ , from the initial  $s^*$  to the  $s^*$  in the exit channel, and (3) at the final  $s^*$  from  $\rho = k\rho_{\text{max}}$  to  $\rho = \rho_{\text{max}}$ . Now all three steps contribute to  $\text{Im} \int p dq$ . For  $k = 1.01$  and  $1.05$ , the values of  $J$  were 3.73 and 4.07, respectively, for the cited  $E$ , thus once again exceeding the value of  $J = 3.65$  for the  $t$ -curve.

These results are summarized in Table I. The path along the  $t$ -curve is the only internally consistent path in Table I: It alone has a zero component of velocity normal to it.

Many other paths can be suggested, and a complete investigation of them would be equivalent to solving Hamilton's equations in the vicinity of the saddle-point. Among the classes of paths are (A3), choosing  $s = 0$  to lie along the bisector of the acute angle in Fig. 1.

$$\rho(s) = [1 \mp a(1 - |s/s^*|)]\rho_{\text{max}}(s) \quad (0 < a < 1). \quad (\text{A3})$$

With the minus sign, one would have  $\rho(s) \leq \rho_{\text{max}}(s)$ , and

TABLE I. Summary of phase integrals along different tunneling paths.

Description of path <sup>a</sup>	$\text{Im} \int p dq / \hbar$
$\rho = 0$ (s-curve)	5.81
$\rho = k \rho_{\text{max}}$ ( $k < 1$ )	> 3.65
$\rho = \rho_{\text{max}}$ (t-curve)	3.65
$\rho = 1.01 \rho_{\text{max}}$	3.73
$\rho = 1.05 \rho_{\text{max}}$	4.07

<sup>a</sup>These paths refer to three-step paths, but only the middle step between  $P$  and  $P'$  is described in this column. The value in the second column is the value of  $\text{Im} \int p dq / \hbar$  for the entire path between  $P$  and  $P'$ . All results are for the SSMK Wall-Porter surface for  $E = 0.3985$  eV.

in the vibrationally-adiabatic approximation the  $\text{Im} p$  in  $J(E)$  would still be the  $p_s$  given by (A2). The  $s$ -distance part of the path length would be greater than that for the  $t$ -curve and so  $J(E)$  would be larger. With the plus sign of (A3),  $\rho(s) \geq \rho_{\text{max}}(s)$ . If one used zero velocity component normal to the path, thereby dropping the vibrational adiabaticity (other than for the  $t$ -curve, for which  $a = 0$ ),  $p$  would be  $[2\mu(E - V)]^{1/2}$ , where  $V$  is the potential energy on the path, and  $J(E)$  could readily be calculated. Calculations for these paths and for other systems will be presented elsewhere.

We have not discussed energies where  $E > V_1(s^\dagger) + E_0(s^\dagger)$  but for which diffraction can occur when  $E$  is just above this barrier. Here, the path which maximizes  $\kappa$  is one for which the end points are imaginary rather than real, and is not, therefore, between  $P$  and  $P'$ . The  $\kappa(E)$  will lie between the values of 0.5 and unity in this region.

<sup>1</sup>E. g., D. G. Truhlar and A. Kuppermann, *J. Am. Chem. Soc.* **93**, 184 (1970); D. G. Truhlar and A. Kuppermann, *Chem. Phys. Lett.* **9**, 269 (1971); G. C. Schatz and A. Kuppermann, *J. Chem. Phys.* **65**, 4668 (1976) and references cited therein; E. Mortensen, *ibid.* **48**, 4029 (1968).

<sup>2</sup>(a) T. F. George and W. H. Miller, *J. Chem. Phys.* **56**, 5722 (1972); (b) *ibid.* **57**, 2458 (1972).

<sup>3</sup>J. R. Stine, Ph.D. Thesis, University of Illinois, 1974.

<sup>4</sup>(a) W. H. Miller, *J. Chem. Phys.* **62**, 1899 (1975); (b) S. Chapman, B. C. Garrett, and W. H. Miller, *J. Chem. Phys.* **63**, 2710 (1975).

<sup>5</sup>S. Glasstone, K. J. Laidler, and H. Eyring, *The Theory of Rate Processes* (McGraw-Hill, New York, 1941), p. 100.

<sup>6</sup>For a reaction of three atoms of masses  $m_1$ ,  $m_2$ , and  $m_3$  in a line, with  $r_1$  denoting the distance between  $m_1$  and  $m_2$  and  $r_2$  denoting the distance between  $m_2$  and  $m_3$ , the coordinates  $x$  and  $y$  in Figs. 1-3 are defined by  $r_1 = x - y \tan \theta$ ,  $r_2 = c y \sec \theta$ , with  $c = [m_1(m_2 + m_3) / m_3(m_1 + m_2)]^{1/2}$  and  $\sin \theta = [m_1 m_3 / (m_1$

$+ m_2)(m_2 + m_3)]^{1/2}$ . Here,  $(\pi/2) - \theta$  denotes the acute angle in Fig. 1. The coordinates  $x$ ,  $y$  have the property that they diagonalize the kinetic energy, and both have a single mass  $\mu$ , in the center of mass system of coordinates, i.e., the kinetic energy in this system is  $(\mu/2)(\dot{x}^2 + \dot{y}^2)$ , with  $\mu = m_1(m_2 + m_3) / (m_1 + m_2 + m_3)$ .

<sup>7</sup>Compare with J. N. L. Connor, *Molec. Phys.* **15**, 37 (1968), Eqs. (14), (15), (18), and (19). The transmission coefficient is the ratio of the transmitted to incident flux, and is calculated from the wave functions in Eqs. (14) and (15), and found to give the present Eq. (2.6). The mapping equations are Eqs. (18) and (19).

<sup>8</sup>R. N. Porter and M. Karplus, *J. Chem. Phys.* **40**, 1105 (1964).

<sup>9</sup>G. C. Schatz and A. Kuppermann (private communication from G. C. Schatz); cf. Fig. 6 of Ref. 4(b); J. W. Duff and D. G. Truhlar, *Chem. Phys. Lett.* **23**, 327 (1973).

<sup>10</sup>(a) D. G. Truhlar and A. Kuppermann, *J. Chem. Phys.* **52**, 3841 (1970); (b) *ibid.* **56**, 2232 (1972).

<sup>11</sup>Reference 10 gives a fit to the results of a calculation of the  $\text{H}_3$  surface in I. Shavitt, R. M. Stevens, F. L. Minn, and M. Karplus, *J. Chem. Phys.* **48**, 2700 (1968) to the functional form given in F. T. Wall and R. N. Porter, *J. Chem. Phys.* **36**, 3256 (1962). The fit is actually to a scaled version of SSMK, scaled as per the suggestion of I. Shavitt, *J. Chem. Phys.* **49**, 4048 (1968).

<sup>12</sup>R. A. Marcus, *J. Chem. Phys.* **45**, 2138 (1966). cf. Eqs. (3) and (4).

<sup>13</sup>For example, (a) M. Born, *Mechanics of the Atom* (Ungar, New York, 1960); (b) J. B. Keller, *Ann. Phys. (N.Y.)* **4**, 180 (1958); (c) R. A. Marcus, *Chem. Phys. Lett.* **7**, 525 (1970); (d) R. A. Marcus, *J. Chem. Phys.* **59**, 5125 (1973); (e) W. H. Miller, *Adv. Chem. Phys.* **25**, 69 (1974) and references cited therein; (f) W. H. Miller, *J. Chem. Phys.* **54**, 5386 (1971); (g) cf. integral expression in W. H. Miller, *J. Chem. Phys.* **53**, 3578 (1970).

<sup>14</sup>(a) J. O. Hirschfelder and E. Wigner, *J. Chem. Phys.* **7**, 616 (1939), who considered a quantum system rather than a trajectory; (b) Nonadiabatic effects in the classical mechanics of reactions are discussed in R. A. Marcus, *J. Chem. Phys.* **45**, 4500 (1966). Vibrational adiabaticity has been used by (c) M. A. Eliason and J. O. Hirschfelder, *ibid.* **30**, 1426 (1959); (d) L. Hofacker, *Z. Naturforsch. Teil A* **18**, 607 (1963); (e) R. A. Marcus, *J. Chem. Phys.* **43**, 1598 (1966), which coined the term "vibrational adiabaticity," and (f) R. A. Marcus, *J. Chem. Phys.* **46**, 959 (1967).

<sup>15</sup>Compare with H. C. Corben and P. Stehle, *Classical Mechanics* (Wiley, New York, 1964), 2nd ed., p. 170 Eq. (57.12)

<sup>16</sup>For example, in Fig. 8 of S. F. Wu and R. A. Marcus, *J. Chem. Phys.* **53**, 4026 (1970), the trajectories for some initial phases are unreactive while others are reactive. The second group thereby has no real-valued  $s^*$ . Unpublished trajectory studies of J. R. Stine in this laboratory showed analogous effects. Compare with R. A. Marcus, *Ber. Bunsenges. Phys. Chem.* **81**, 190 (1977) for a qualitative discussion of nonadiabatic effects.

<sup>17</sup>R. A. Marcus, Ref. 13(f) cf. Ref. 13(b).

<sup>18</sup>Judging from the results near  $\kappa(E) = 0.5$ , these effects appear to be larger for the Porter-Karplus surface than for the Wall-Porter one.

<sup>19</sup>H. S. Johnston and D. Rapp, *J. Am. Chem. Soc.* **83**, 1 (1961).